

## Evidence for 2D-Network Structure of Monolayer Silica Film on Mo(112)

J. Seifert, D. Blauth, and H. Winter\*

*Institut für Physik, Humboldt Universität zu Berlin, Brook-Taylor-Str. 6, D-12489 Berlin-Adlershof, Germany*

(Received 26 March 2009; published 1 July 2009)

The structure of a monolayer silica film on a Mo(112) surface is investigated by grazing scattering of 25 keV  $H^0$  atoms. By detection of the number of projectile induced emitted electrons as function of azimuthal angle of rotation of the target surface, the geometrical structure of atoms forming the topmost layer of the silica film is determined via ion beam triangulation. From our data we find evidence for the arrangement of surface atoms in terms of a two-dimensional Si-O-Si network model.

DOI: 10.1103/PhysRevLett.103.017601

PACS numbers: 79.20.Rf, 68.55.-a, 68.60.-p, 81.15.-z

Thin oxide films deposited on metal surfaces have interesting applications as insulating layers in electronic devices, protective films, or as substrate for the deposition of nanoparticles in catalysis [1,2]. In the latter case, such defined films are important prerequisites for detailed studies on the relation between their geometrical structure and reactivity, where the good electric and thermal conductivity avoids the charging problem in many surface analytical tools using bulk oxide crystals. On the other hand, materials with reduced dimensionality might have different properties compared to the bulk. Silica ( $SiO_2$ ) is an oxide which is widely used in catalytic applications so that the preparation of ultrathin crystalline films is of interest. Monolayer thick silica films can be prepared on a Mo(112) substrate via reactive epitaxial growth of Si on oxygen under UHV conditions [3,4]. In recent years, considerable efforts were undertaken in order to clear up the structure of those films based on established surface analytical tools as scanning tunneling microscopy (STM), infrared absorption spectroscopy (IRAS), x-ray photoelectron spectroscopy (XPS), or high resolution electron energy loss spectroscopy (HREELS). From the theoretical side, structural models were proposed from calculations based on density functional theory (DFT). Also interesting features for the calculated electronic structure of the film have been reported [5].

Basically, two different models for the structure of the silica film are presently discussed. Goodman and co-workers [6–8] proposed for this film a layer of isolated  $SiO_4$  clusters arranged in a  $c(2 \times 2)$  pattern on Mo(112) where all oxygen atoms bond to Mo atoms of the substrate [9]. On the other hand, a two-dimensional honeycombl-like network of  $SiO_4$  tetrahedra was suggested [4,10–12]. In this latter model, only one O atom binds to a Mo atom of the substrate, whereas the three further O atoms form Si-O-Si bonds with neighboring tetrahedra (see sketch in Fig. 1). Until today, there is a controversy on these two different structural models [13,14], and in a recent review it was stated that “the detailed structure of monolayer  $SiO_2$ /Mo(112) is still an issue yet to be resolved” [8].

In this Letter we will focus on this problem and present experimental work based on ion scattering which provides clear cut evidence for the structural model of the silica/Mo(112) system. Our studies are based on an ion beam triangulation (IBT) method performed with fast hydrogen atoms scattered under a grazing angle of incidence from the film surface [15] where information on the geometrical arrangement of atoms in the topmost layer of the film is derived in a straightforward manner. From a direct comparison of the two conflicting structural models with our experiments based on classical trajectory computer simulations we conclude that only for the two-dimensional network model the arrangement of topmost atoms of the silica film is consistent with the data.

In the experiments we have scattered neutral H atoms with an energy of 25 keV from a clean Mo(112) surface and from the surface of a silica film grown on the Mo(112) substrate under grazing angles of incidence  $\Phi_{in} \leq 1$  deg. The fast neutral beams were produced via neutralization of ions in a gas cell in front of our UHV chamber (base pressure some  $10^{-11}$  mbar). The Mo(112) target surface was prepared by cycles of grazing sputtering with 25 keV  $Ar^+$  ions and subsequent annealing via heating (bombardment of the rear of the Mo target with 1.3 keV electrons) to about 1900 K. Initial contaminations with carbon atoms were removed via cycles of oxidation and annealing. Sharp

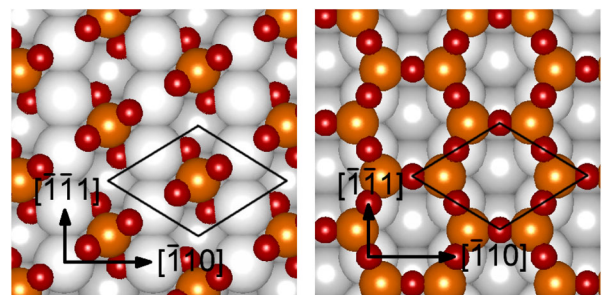


FIG. 1 (color online). Sketch for positions of atoms in cluster model (left panel) and 2D-network model (right panel). Red/black symbols: O atoms, orange/gray symbols: Si atoms, white symbols: Mo atoms.

LEED patterns for the Mo(112) surface are observed with a SPALEED system (Omicron Nanotechnology). The silica films were produced with an electron evaporator EFM3 (Omicron Nanotechnology) charged with a Si rod of 2 mm in diameter following the recipes given by Kaya *et al.* [16]. The evaporation rate of Si atoms was about 0.25 monolayers (ML) per minute. After initial oxidation of Mo(112), 1.2 ML of Si were deposited at 900 K at a partial oxygen pressure of  $5 \times 10^{-8}$  mbar. Thereafter the film was annealed between 1100 and 1250 K for about 5 min. For such films sharp LEED patterns showing a  $c(2 \times 2)$  structure are observed.

The structure of the clean Mo(112) substrate and, in particular, of the monolayer silica film is studied via a recent variant of ion beam triangulation (IBT) [17,18] where emitted electrons are detected by means of a surface barrier detector (SBD) biased to 25 kV. Electrons emitted from the surface are accelerated onto the entrance aperture of the detector and produce in the barrier region numbers of electron hole pairs proportional to the energy of the impinging electrons. Owing to the pile up of the resulting output pulses from electrons created in a single atom impact event at the target, the pulse heights of the SBD scale directly with the number of electrons per atom impact [19,20]. Therefore the electron number distribution (END) can be derived from the pulse height distribution of the SBD. This distribution peaks at about the mean number of electrons emitted during the collisions of atoms with the surface (total yield) which amounts to about 5 electrons here.

Scattering experiments from surfaces under grazing impact are performed in the regime of surface channeling [21,22], i.e., a steering of projectiles by atoms of the topmost surface layer. The key feature of the triangulation method applied here is related to the modification of projectile induced electron emission for the transition from *planar* to *axial surface channeling* [15,23]. Whenever the direction of the incident projectile beam coincides with a low indexed azimuthal direction in the surface plane, the projectiles are steered along strings of atoms and approach the topmost surface layer closer than under a random orientation with respect to those strings (*planar channeling*). This change for the trajectories is accompanied by an enhanced number of electrons emitted for scattering under *axial channeling*. Then the number of events accompanied with the emission of low numbers of electrons is reduced, since the distribution is shifted towards higher electron numbers.

In the experiments, the discriminator levels are set to low pulse heights for the output of the SBD. This signal shows dips, whenever the fast projectiles are steered along atomic strings in the surface plane. Owing to this steering, the method shows an extreme sensitivity to the topmost surface layer. Since for grazing impact of 25 keV H atoms on a solid surface total electron yields clearly exceed one,

each projectile generates a pulse. The maximum count rate of the detector system of about  $10^4$  counts per second corresponds to a flux of incident H atoms equivalent to a current in the sub-fA regime. Thus radiation damage caused by projectiles can be fully neglected. More details concerning this method are given elsewhere [17,18].

In Fig. 2 we show triangulation curves, i.e., the counts of the SBD related to the emission of about 3 to 5 electrons as function of the azimuthal angle of rotation of the target surface, for scattering of 25 keV H atoms under  $\Phi_{in} = 0.9$  deg from a clean Mo(112) surface (black solid curve) and from a 1 ML silica film grown on a Mo(112) substrate (solid gray/red curve). The curves reveal dips, whenever the fast atoms are scattered along prominent axial channels formed by strings of atoms of the topmost surface layer of metal substrate or oxide film. The most prominent dips in both curves can be ascribed to low indexed directions of the two-dimensional lattice of the Mo(112) surface, e.g., [10] at  $0^\circ$  (corresponds to  $[\bar{1} \bar{1} 1]$  for bulk crystal), [31] at  $28.6^\circ$ , [21] at  $39.2^\circ$ , [11] at  $58.5^\circ$ , and [01] ( $[\bar{1} 1 0]$ ) at  $90^\circ$ . Striking feature for the data of the silica film is the appearance of prominent dips at higher indexed directions which are weak or absent in the curve for the clean substrate.

In order to test the experimental triangulation curve with respect to the two controversial structural models, we performed trajectory computer simulations based on classical mechanics. The scattering potential for the projectiles is obtained from the superposition of interatomic pair potentials in the Thomas-Fermi approach as proposed by O'Connor and Biersack [24]. The probability for emission of electrons is directly related to the electron density of surface atoms which is assumed to decay exponentially from the center. From the summation of electron emission events over complete trajectories we derive electron num-

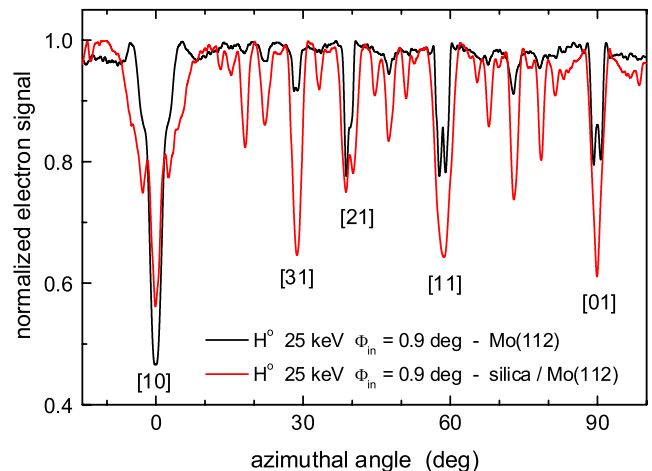


FIG. 2 (color online). Triangulation curve (events related to emission of 3 to 5 electrons as function of azimuthal angle) for scattering of 25 keV H atoms under  $\Phi_{in} = 0.9^\circ$ . Solid black curve: clean Mo(112), solid grey (red) curve: silica film on Mo(112).

ber distributions for each azimuthal angle. Selection of events for an interval of electron numbers as in the experiments allows us to compare the calculations directly with the measurements.

In Figs. 3 and 4 we have plotted the experimental triangulation curve for the silica film on Mo(112) as shown already in Fig. 2 for comparison with the computer simulations for the cluster (Fig. 3) and the 2D-network model (Fig. 4). This analysis reveals for the cluster model (two domains of mirror symmetry for the  $c(2 \times 2)$  unit cell are taken into account) pronounced deviations, in particular, for several higher indexed axial channels, whereas the simulations for the 2D-network structural model reproduces even fine details of the experimental curve. In view of the simplifying approximations for the complex electron excitation and emission processes, the agreement of the simulations based on the 2D-network model with the data is excellent. All relevant axial channels, present in the measurements, are reproduced, and also the depths of the dips, which can be considered as a measure for the widths of the axial channels, are in accord with the data. From this good agreement and the evident failure of the cluster model (holds also for its former version in [6]) in reproducing the experimental curve, we conclude that the structure of the silica film has to be very close to the proposed model of the 2D network. The clear cut signature of the triangulation method probing the long range ordering of the topmost layer of surface atoms with extreme sensitivity thus provides an important contribution to clear up the controversy based on investigations via STM, infrared absorption, and DFT calculations.

Aside from detailed tests on the structural models based on elaborate computer simulations, key features on the structures can be deduced from simple geometrical arguments. For the present problem, it is straightforward to find signatures which disprove the cluster model. Comparing

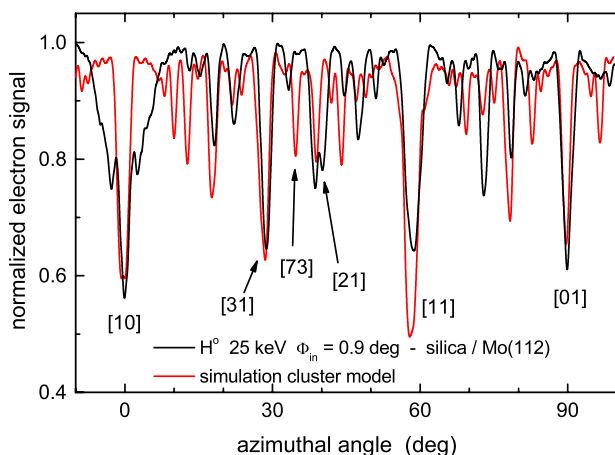


FIG. 3 (color online). Triangulation curve for scattering of 25 keV H atoms under  $\Phi_{in} = 0.9^\circ$ . Solid black curve: silica film on Mo(112), gray/red curve: simulation based on cluster model.

the simulations in Figs. 3 and 4 reveals for the cluster model pronounced dips which are neither observed in the experiments nor in the simulations based on the 2D-network model. Such dips are located at azimuthal angles of, e.g.,  $10.2^\circ$ ,  $35.0^\circ$ , and  $83.0^\circ$  which correspond to [91], [73], and [15] directions, respectively. The presence of these dips for the cluster model can be understood by the arrangement of the topmost O atoms which occupy positions close to  $(1/4, 1/4)$  and  $(3/4, 3/4)$  in the surface unit cell of the Mo substrate as sketched in the upper part of Fig. 5. As an example, we have highlighted in Fig. 5 for the cluster model (upper figure) and for the 2D-network model (lower figure) the [73] axial channel formed by topmost O atoms. It is evident that this high indexed channel is doubled in width for the cluster model so that axial surface channeling can take place giving rise to dips in the simulated triangulation curves. For the 2D-network model the [73] channels are too narrow to observe a transition from planar (random alignment) to axial channeling and almost no dip for this azimuthal direction is observed. This is in accord with the measurements.

On the other hand, in the 2D-network model the O atoms of the topmost layer occupy the same lateral positions as substrate atoms (cf. Figs. 1 and 5) so that positions of dips in the triangulation curves for the Mo substrate and the silica film are the same (cf. Fig. 2). Owing to the weaker H-O compared to the H-Mo interatomic potentials, the projectiles penetrate deeper into the axial channels resulting in more pronounced dips in the triangulation curve for silica. However, instead of a monotonic increase of the dips from the [31], [21], to the [11] directions of the clean Mo surface, we observe a reduced signal along [21] for silica. This can be understood from the 2D network by lower lying O atoms which block projectiles from penetration into the [21] channel opposite to scattering along

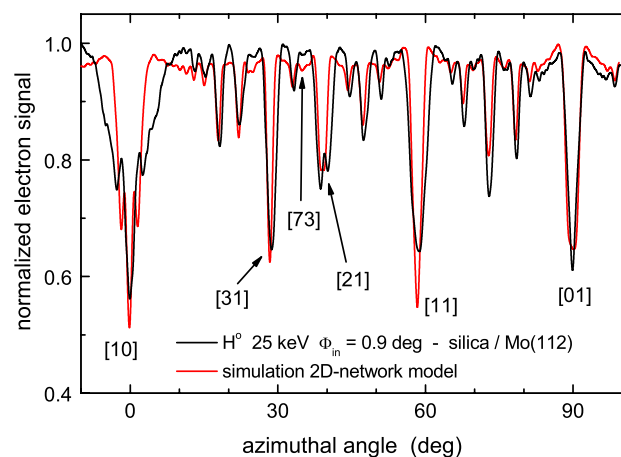


FIG. 4 (color online). Triangulation curve for scattering of 25 keV H atoms under  $\Phi_{in} = 0.9^\circ$ . Solid black curve: silica film on Mo(112), gray/red curve: simulation based on 2D-network model.

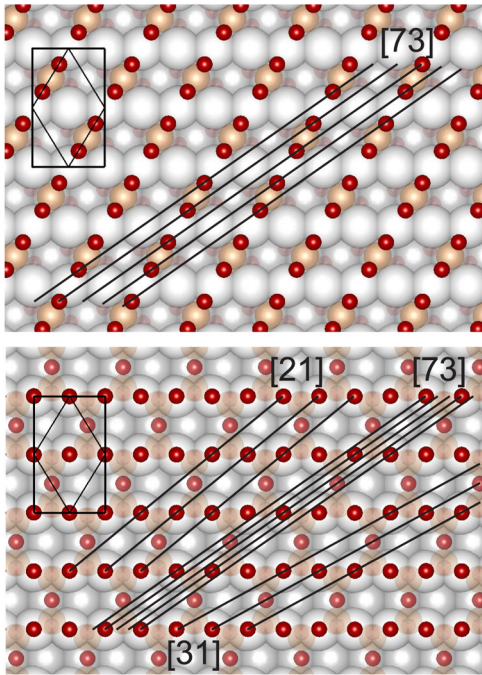


FIG. 5 (color online). Sketch of positions of topmost layer atoms for cluster model (upper panel) and 2D-network model (lower panel). Solid lines indicate [21], [73] and [31] channels. Red/black symbols: O atoms of topmost layer, light red/gray symbols: O atoms in lower layer, white symbols: Mo atoms.

[31] (cf. Fig. 5). More details on this topic will be given in a forthcoming paper.

In conclusion, we have studied the structure of a 1 ML silica film on Mo(112) via a variant of ion beam triangulation where emitted electrons are detected. The output signal of the detector shows pronounced dips, whenever the projectile beam is scattered along defined channels formed by strings of atoms in the topmost surface layer. This signal as function of the azimuthal angle of rotation shows pronounced dips which are well reproduced in depths and positions by computer simulations based on the 2D-network structural model for the silica film. For the cluster model, we find considerable discrepancies with the measurements. Thus, our work is in clear favor for the 2D-network model as the appropriate structure.

We thank the Sfb546 for financial support, K. Maass and G. Lindenberg for their assistance in the preparation of the experiments, Dr. M. Sierka and M. Baron for helpful discussions.

\*Author to whom correspondence should be addressed.  
winter@physik.hu-berlin.de

- [1] H. J. Freund, *Faraday Discuss.* **114**, 1 (1999).
- [2] W. D. Goodman, *J. Catal.* **216**, 213 (2003).
- [3] T. Schroeder, M. Adelt, B. Richter, M. Naschitzki, M. Bäumer, and H. J. Freund, *Surf. Rev. Lett.* **7**, 7 (2000).
- [4] J. Weissenrieder, S. Kaya, J. L. Lu, H. J. Gao, S. Shaikhutdinov, H. J. Freund, M. M. Sierka, T. K. Todorova, and J. Sauer, *Phys. Rev. Lett.* **95**, 076103 (2005).
- [5] C. Freysoldt, P. Rinke, and M. Scheffler, *Phys. Rev. Lett.* **99**, 086101 (2007).
- [6] M. Chen, A. K. Santra, and D. W. Goodman, *Phys. Rev. B* **69**, 155404 (2004).
- [7] M. Chen and D. W. Goodman, *Surf. Sci.* **600**, L255 (2006).
- [8] M. S. Chen and D. W. Goodman, *J. Phys. Condens. Matter* **20**, 264013 (2008).
- [9] I. N. Yakovkin, *Surf. Rev. Lett.* **12**, 449 (2005).
- [10] L. Giordano, D. Ricci, G. Pacchioni, and P. Ugliengo, *Surf. Sci.* **584**, 225 (2005).
- [11] T. K. Todorova, M. Sierka, J. Sauer, S. Kaya, J. Weissenrieder, J. L. Lu, H. J. Gao, S. Shaikhutdinov, and H. J. Freund, *Phys. Rev. B* **73**, 165414 (2006).
- [12] M. Sierka, T. K. Todorova, S. Kaya, D. Stacchiola, J. Weissenrieder, J. L. Lu, H. J. Gao, S. Shaikhutdinov, and H. J. Freund, *Chem. Phys. Lett.* **424**, 115 (2006).
- [13] L. Giordano, D. Ricci, G. Pacchioni, and P. Ugliengo, *Surf. Sci.* **601**, 588 (2007).
- [14] M. Chen and D. W. Goodman, *Surf. Sci.* **601**, 591 (2007).
- [15] R. Pfandzelter, T. Bernhard, and H. Winter, *Phys. Rev. Lett.* **90**, 036102 (2003).
- [16] S. Kaya, M. Baron, D. Stacchiola, J. Weissenrieder, S. Shaikhutdinov, T. K. Todorova, M. Sierka, J. Sauer, and H. J. Freund, *Surf. Sci.* **601**, 4849 (2007).
- [17] T. Bernhard, M. Baron, M. Gruyters, and H. Winter, *Phys. Rev. Lett.* **95**, 087601 (2005).
- [18] T. Bernhard, J. Seifert, and H. Winter, *J. Phys. Condens. Matter* **21**, 134001 (2009).
- [19] G. Lakits, F. Aumayr, and H. Winter, *Rev. Sci. Instrum.* **60**, 3151 (1989).
- [20] F. Aumayr, G. Lakits, and H. Winter, *Appl. Surf. Sci.* **47**, 139 (1991).
- [21] D. Gemmell, *Rev. Mod. Phys.* **46**, 129 (1974).
- [22] H. Winter, *Phys. Rep.* **367**, 387 (2002).
- [23] H. Winter, K. Maass, S. Lederer, H. P. Winter, and F. Aumayr, *Phys. Rev. B* **69**, 054110 (2004).
- [24] D. J. O'Connor and J. Biersack, *Nucl. Instrum. Methods Phys. Res., Sect. B* **15**, 14 (1986).